Asian Journal of Chemistry; Vol. 38, No. 9 (2026), 2341-2355
ASIAN JOURNAL OF CHEMISTRY
https://doi.org/10.14233/ajchem.2026.36440

Efficient Removal of Methylene Blue Dye and Ofloxacin Antibiotic using Eggshell Waste as Adsorbent

SARAPEE CHUNKAEW[1], SOMPORN RUANG-ON[1] and PRAWIT NUENGMATCHA[1,2,*]

[1]Creative Innovation in Science and Technology, Faculty of Science and Technology, Nakhon Si Thammarat Rajabhat University, Nakhon Si Thammarat, 80280, Thailand
[2]Center of Excellence in Nanomaterials Chemistry, Faculty of Science and Technology, Nakhon Si Thammarat Rajabhat University, Nakhon Si Thammarat, 80280, Thailand

*Corresponding author: E-mail: prawit_nue@nstru.ac.th

Received: 15 May 2026 *Accepted*: 31 July 2026 *Published online*: 5 September 2026 AJC-22462

Eggshell waste, an inexpensive and abundant material, serves as an eco-friendly adsorbent for wastewater treatment. This study evaluates its efficiency in removing methylene blue (MB) dye and ofloxacin (OFX) antibiotic from aqueous solutions. The adsorbent was characterized by Fourier-transform infrared spectroscopy (FT-IR), scanning electron microscopy (SEM) and energy-dispersive X-ray spectroscopy (EDS) to assess its surface morphology and composition. Batch adsorption experiments identified the optimal conditions as 0.04 g of adsorbent, a contact time of 120 min, an initial MB concentration of 4 mg/L and an initial OFX concentration of 6 mg/L. Under these conditions, the removal efficiencies reached 73.01% for MB and 85.34% for OFX, with maximum adsorption capacities of 9.95 mg/g and 0.93 mg/g, respectively. Methylene blue (MB) dye adsorption was strongly affected by solution pH and electrostatic interactions, whereas OFX adsorption involved electrostatic attraction, hydrogen bonding and surface complexation. Kinetic studies revealed that MB adsorption followed a multi-step diffusion mechanism, while OFX adsorption was best described by the pseudo-second-order kinetic model. Thermodynamic analysis indicated that the adsorption of both pollutants was spontaneous and endothermic, accompanied by positive entropy changes. The adsorbent exhibited good regeneration performance, retaining more than 50% of its MB and OFX removal efficiencies after five adsorption-desorption cycles. These findings demonstrate that the eggshell waste calcined at 600 ºC is an efficient, reusable and sustainable adsorbent with considerable potential for the treatment of dye- and antibiotic contaminated wastewater.

Keywords: Eggshell waste, Methylene blue, Ofloxacin, Adsorption.

INTRODUCTION

Water pollution from organic dyes and pharmaceutical residues poses a critical global challenge due to their persistence, toxicity and resistance to conventional treatments [1,2]. Methylene blue (MB), a cationic dye widely used in textiles and industry, is a known carcinogen harmful to humans and aquatic life [3]. Similarly, ofloxacin (OFX), a fluoroquinolone antibiotic prevalent in wastewater, risks bioaccumulation and fosters antibiotic-resistant bacteria [4]. The coexistence of dyes and antibiotics complicates remediation, demanding efficient, sustainable technologies.

Conventional methods like coagulation [5], advanced oxidation processes [6], nanofiber membranes [7] and biodegradation [8], often involve high costs, secondary pollution or operational complexity. In contrast, adsorption is considered an effective treatment method because of its simplicity, low cost, and high efficiency. Its performance largely depends on the properties of the adsorbent, leading to increasing interest in the development of low-cost, eco-friendly adsorbents derived from waste materials [9,10].

The valorization of agricultural and biogenic wastes has gained increasing attention as a sustainable approach to environmental remediation [11]. Eggshell waste, composed mainly of calcium carbonate with small amounts of organic matter, possesses a porous structure and surface functional groups that make it a suitable adsorbent [12]. Its utilization not only reduces the burden of solid waste disposal but also provides a low-cost alternative to conventional adsorbents such as activated carbon. Although eggshell-derived materials have been reported for the removal of various pollutants [13-15], studies on the adsorption of both dyes and antibiotics using

raw eggshell waste remain limited. In particular, information on the removal of methylene blue (MB) and ofloxacin (OFX), including optimization of adsorption conditions and evaluation of adsorption capacity, is still scarce.

This study investigates the use of raw eggshell waste as a low-cost adsorbent for the removal of MB and OFX from aqueous solutions. The adsorbent was characterized using Fourier-transform infrared spectroscopy (FT-IR), scanning electron microscopy (SEM) and energy-dispersive X-ray spectroscopy (EDS). The effects of adsorbent dosage, contact time and initial pollutant concentration on adsorption performance were systematically evaluated to determine the optimum conditions. Removal efficiency and adsorption capacity were used to assess the performance of the adsorbent. The findings of this study contribute to the development of sustainable wastewater treatment technologies through the utilization of waste materials within a circular economy framework.

EXPERIMENTAL

All chemicals used were of analytical (AnalaR) grade and obtained from commercial suppliers without further purification. Eggshell waste was washed with distilled water, dried in an oven at 105 ºC, ground and sieved to 0.5-2.0 mm particle size. Portions were then calcined in a furnace at 400, 600 and 800 ºC.

Characterization: The morphology of the samples was examined using scanning electron microscopy (SEM; Quanta 400, Thermo-Fisher Scientific). Elemental composition was determined by energy-dispersive X-ray spectroscopy (EDS). Fourier-transform infrared (FT-IR) spectra were recorded on an EQUINOX 55 spectrometer (Bruker, Germany) at room temperature over 4000-450 cm^{-1}.

Adsorption experiments: Batch adsorption experiments were conducted to determine the optimum conditions for the removal of methylene blue (MB) and ofloxacin (OFX). The effects of initial pollutant concentration (1-10 mg/L), adsorbent dosage (0.005-0.12 g), contact time (0-180 min) and solution pH (1-11) were investigated. A known amount of adsorbent was added to 50 mL of MB or OFX solution in 125 mL conical flasks and shaken at 150 rpm at room temperature. After adsorption, the suspensions were centrifuged for 10 min and the residual concentrations of MB and OFX were determined using a UV-Vis spectrophotometer at 665 and 281 nm, respectively. All the experiments were performed in triplicate. The adsorption capacity at equilibrium (q_e, mg/g) and removal efficiency (%) were calculated using eqns. 1 and 2, respectively [16,17].

$$q_e = \frac{V(C_o - C_e)}{m} \quad (1)$$

$$\text{Removal (\%)} = \frac{C_o - C_e}{C_o} \times 100 \quad (2)$$

where C_o is the MB/OFX initial concentration (mg/L), C_e is the MB/OFX concentration (mg/L) at the equilibrium state, V is the solution volume (L) and m is the adsorbent mass (g).

Adsorption isotherms: Equilibrium isotherm studies predict adsorbate behaviour and fit experimental data to models like Langmuir and Freundlich [17]. The linearized Langmuir model is:

$$\frac{C_e}{q_e} = \frac{C_e}{q_m} + \frac{1}{q_m K_L} \quad (3)$$

$$\log q_e = \log K_F + \frac{1}{n}\log C_e \quad (4)$$

where q_m stands for the highest concentration of MB/OFX absorbed per adsorbent weight unit (mg/g); C_e stands for the concentration of MB/OFX at equilibrium (mg/L); q_e for the quantity of MB/OFX absorbed per unit weight of the adsorbent at equilibrium and K_L for the Langmuir constant (L/mg). The values of q_m and K_L were calculated using the slopes and intercepts of the C_e/q_e *vs.* C_e plots, respectively. While the adsorption intensity is denoted by n and the Freundlich constant by K_F. The values of K_F and 1/n (between 0 and 1) were found using the linear plots of log q_e *versus* log C_e.

pH_{pzc} studies: The point of zero charge (pH_{PZC}) of raw and calcined eggshell powders (400, 600 and 800 ºC) was determined using the pH drift method. Briefly, 0.1 g of adsorbent was added to 50 mL of 0.1 M NaCl solution with initial pH values adjusted to 1, 3, 5, 7, 9 and 11 using 0.1 M HCl or 0.1 M NaOH. The suspensions were shaken at 150 rpm for 24 h at room temperature, after which the final pH was measured. The pH_{PZC} was determined from the plot of ΔpH (pH_{final} − $pH_{initial}$) *versus* initial pH, where ΔpH = 0.

Adsorption kinetic study: Adsorption kinetic experiments were conducted to investigate the adsorption rates and possible rate-controlling mechanisms of methylene blue (MB) and ofloxacin (OFX) onto adsorbents. The experiments were performed using eggshell powders calcined at 600 ºC. An accurately weighed amount of 0.04 g of each adsorbent was added to a 125 mL Erlenmeyer flask containing 50 mL of MB or OFX solution. The initial concentrations of MB and OFX were maintained at 4 and 6 mg/L, respectively. The mixtures were agitated at 150 rpm and room temperature for predetermined contact times of 0, 30, 60, 90, 120, 150 and 180 min. After each adsorption period, the adsorbent was separated by centrifugation for 10 min. The residual concentrations of MB and OFX in the supernatant were determined using a UV-Vis spectrophotometer at maximum wavelengths of 665 and 281 nm, respectively.

The pseudo-first-order kinetic model assumes that the adsorption rate is proportional to the number of unoccupied adsorption sites on the adsorbent surface. The model is expressed in its linear form as follows:

$$\log(q_e - q_t) = \log q_e - \frac{k_1}{2.303} t \quad (5)$$

where q_e and q_t are the adsorption capacities at equilibrium and at time t, respectively (mg/g), k_1 is the pseudo-first-order rate constant (min^{-1}) and t is the contact time (min). The values of k_1 and calculated equilibrium adsorption capacity, q_e, were obtained from the slope and intercept of the linear plot of log (q_e–q_t) *versus* t.

The pseudo-second-order kinetic model assumes that the adsorption rate depends on the availability of adsorption sites and the square of the number of unoccupied sites. The linear form of the pseudo-second-order kinetic model is expressed as:

$$\frac{t}{q_t} = \frac{1}{k_2 q_e^2} + \frac{t}{q_e} \quad (6)$$

where k_2 is the pseudo-second-order rate constant expressed in g mg^{-1} min^{-1}, while q_e, q_t and t have the same meanings defined previously. The values of q_e and k_2 were calculated from the slope and intercept of the plot of t/q_t *versus* t, respectively.

The Weber-Morris intraparticle diffusion model was applied to determine whether the diffusion of MB and OFX molecules within the pores of the eggshell adsorbent was the rate-controlling step. The model is expressed as:

$$q_t = k_{id} t^{1/2} + C \quad (7)$$

where k_{id} is the intraparticle diffusion rate constant expressed in mg g^{-1} $min^{-1/2}$, $t^{1/2}$ is the square root of contact time and C is the intercept related to the thickness of the boundary layer. The values of k_{id} and C were obtained from the slope and intercept of the plot of q_t *versus* $t^{1/2}$, respectively.

Thermodynamic study: Thermodynamic experiments were conducted using only the eggshell powder calcined at 600 ºC, since this adsorbent exhibited the highest removal efficiency and adsorption capacity for both methylene blue (MB) and ofloxacin (OFX) among the tested eggshell materials. An accurately weighed amount of 0.04 g of the 600 ºC-calcined eggshell powder was added to a 125 mL Erlenmeyer flask containing 50 mL of MB or OFX solution. The initial concentrations of MB and OFX were 4 and 10 mg/L. The adsorption experiments were performed at controlled temperatures of 15, 30 and 45 ºC, corresponding to 288.15, 303.15 and 318.15 K, respectively.

The mixtures were agitated in a temperature-controlled orbital shaker at 150 rpm for 120 min, which was previously identified as the equilibrium contact time. After adsorption, the suspensions were centrifuged for 10 min to separate the adsorbent from the solution. The residual concentrations of MB and OFX were determined using a UV-Vis spectrophotometer at maximum wavelengths of 665 and 281 nm, respectively. All experiments were performed in triplicate and the average values were used for thermodynamic calculations.

The standard Gibbs free-energy change was calculated using:

$$\Delta G^o = RT \ln K_c \quad (8)$$

where ΔG^o is the standard Gibbs free-energy change (J/mol); R is the universal gas constant (8.314 J/mol K); T is the absolute temperature (K) and K_c is the dimensionless equilibrium constant. The calculated ΔG^o values were converted to kJ/mol by dividing by 1,000. A negative ΔG^o value indicates that adsorption is spontaneous, while a positive value indicates a non-spontaneous process under the investigated conditions.

The standard enthalpy change (ΔH^o) and standard entropy change (ΔS^o) were determined using the van't Hoff equation:

$$\ln K_c = \frac{\Delta S^o}{R} - \frac{\Delta H^o}{RT} \quad (9)$$

A plot of $\ln K_c$ *versus* 1/T was constructed. The thermodynamic parameters were obtained from the slope and intercept of the linear plot:

$$\text{Slope} = -\frac{\Delta H^o}{R}$$

$$\text{Intercept} = \frac{\Delta S^o}{R}$$

Therefore:

$$\Delta H^o = -\text{Slope} \times R$$

$$\Delta S^o = \text{Intercept} \times R$$

where ΔH^o is expressed in J/mol or kJ/mol and ΔS^o is expressed in J/mol K.

The relationship between the three thermodynamic parameters can also be expressed as:

$$\Delta G^o = \Delta H^o - T\Delta S^o \quad (10)$$

RESULTS AND DISCUSSION

FTIR analysis: The FTIR spectra of raw and calcined eggshell waste are shown in Fig. 1. The spectrum of the raw eggshell displays a broad absorption band at 3600-3400 cm^{-1}, which is assigned to O–H stretching vibrations of adsorbed water and hydroxyl groups [18]. Strong bands at 1450-1400, 870 and 710 cm^{-1} are attributed to the characteristic vibrations of carbonate (CO_3^{2-}), reflecting the predominance of calcium carbonate ($CaCO_3$) in the raw eggshell [18,19].

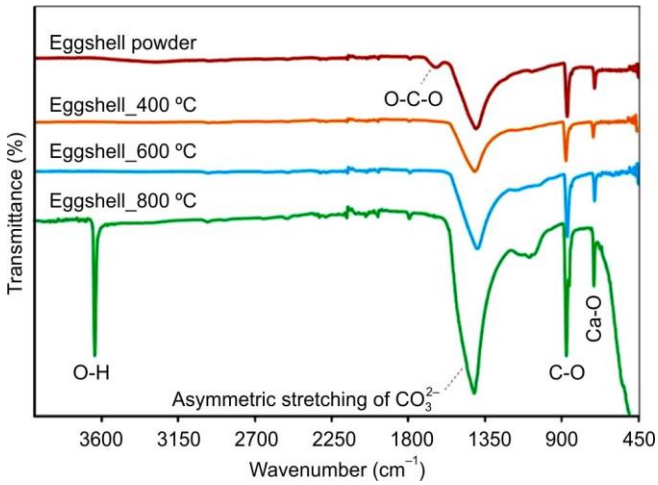

Fig. 1. FTIR spectra of raw eggshell powder and eggshell powders calcined at 400, 600 and 800 ºC

Calcination at 400 and 600 ºC reduced the intensity of the carbonate bands, accompanied by partial decomposition of $CaCO_3$ and removal of organic matter. The O–H band also became weaker following the loss of physically adsorbed water and volatile species. At 600 ºC, the spectrum represents an intermediate stage where decomposition of $CaCO_3$ had started, while much of the carbonate framework remained intact. Calcination at 800 ºC caused a marked decrease in the carbonate bands, accompanied by the appearance of new bands in the 600-500 cm^{-1} region. These bands are assigned to Ca–O vibrations and confirm the formation of CaO after thermal decomposition of $CaCO_3$ [19]. The conversion of $CaCO_3$ into CaO changed the surface chemistry of the material by increasing its basic character, which favours interactions with pollutant molecules.

FTIR analysis further confirms that calcination temperature has a strong influence on the chemical structure of eggshell waste. The decrease in hydroxyl and carbonate groups, together with the formation of CaO, modifies the surface properties of the adsorbent. These observations agree with the SEM and EDS results and explain the improved adsorption behaviour toward methylene blue and ofloxacin through electrostatic interactions and surface complexation.

SEM analysis: SEM images of raw and calcined eggshell waste are shown in Fig. 2a-d. The raw eggshell (Fig. 2a) exhibits a dense and compact structure composed of irregular particles with rough surfaces and limited porosity, characteristics that restrict the number of available adsorption sites. Calcination at 400 ºC (Fig. 2b) breaks the compact structure and introduces microcracks and small voids through the decomposition of organic matter and the release of volatile components, marking the onset of pore development.

The sample calcined at 600 ºC (Fig. 2c) exhibits a highly porous surface with well-dispersed granular particles, numerous pores and superior surface roughness. These structural features provide more accessible active sites for the adsorption of methylene blue (MB) and ofloxacin (OFX). At 800 ºC (Fig. 2d), particle agglomeration and sintering become evident, accompanied by pore collapse and pore merging, which compact the structure and reduce the available surface area [20]. The micrographs identify 600 ºC as the most suitable calcination temperature, where the porous structure and surface texture are most favourable for pollutant adsorption.

EDS analysis: Energy-dispersive X-ray spectroscopy (EDS) was used to examine the elemental composition of raw and calcined eggshell waste (Fig. 3a-d). The EDS spectrum of the raw eggshell (Fig. 3a) is dominated by calcium (Ca), oxygen (O) and carbon (C), consistent with $CaCO_3$ as the major constituent, together with small amounts of magnesium (Mg) and sulfur (S). After calcination at 400 ºC (Fig. 3b), the carbon content decreases slightly as organic matter decomposes, increasing the relative proportions of Ca and O. The sample calcined at 600 ºC (Fig. 3c) contains still less carbon and higher Ca and O contents, leaving a surface with a higher number of accessible adsorption sites [21].

Calcination at 800 ºC (Fig. 3d) exhibit only a small carbon signal, while Ca and O become the predominant elements. This composition is characteristic of the thermal decomposition of $CaCO_3$ to CaO with the release of CO_2 [19]. The formation of CaO changes the surface chemistry and favours interactions between the adsorbent and pollutant molecules through electro-

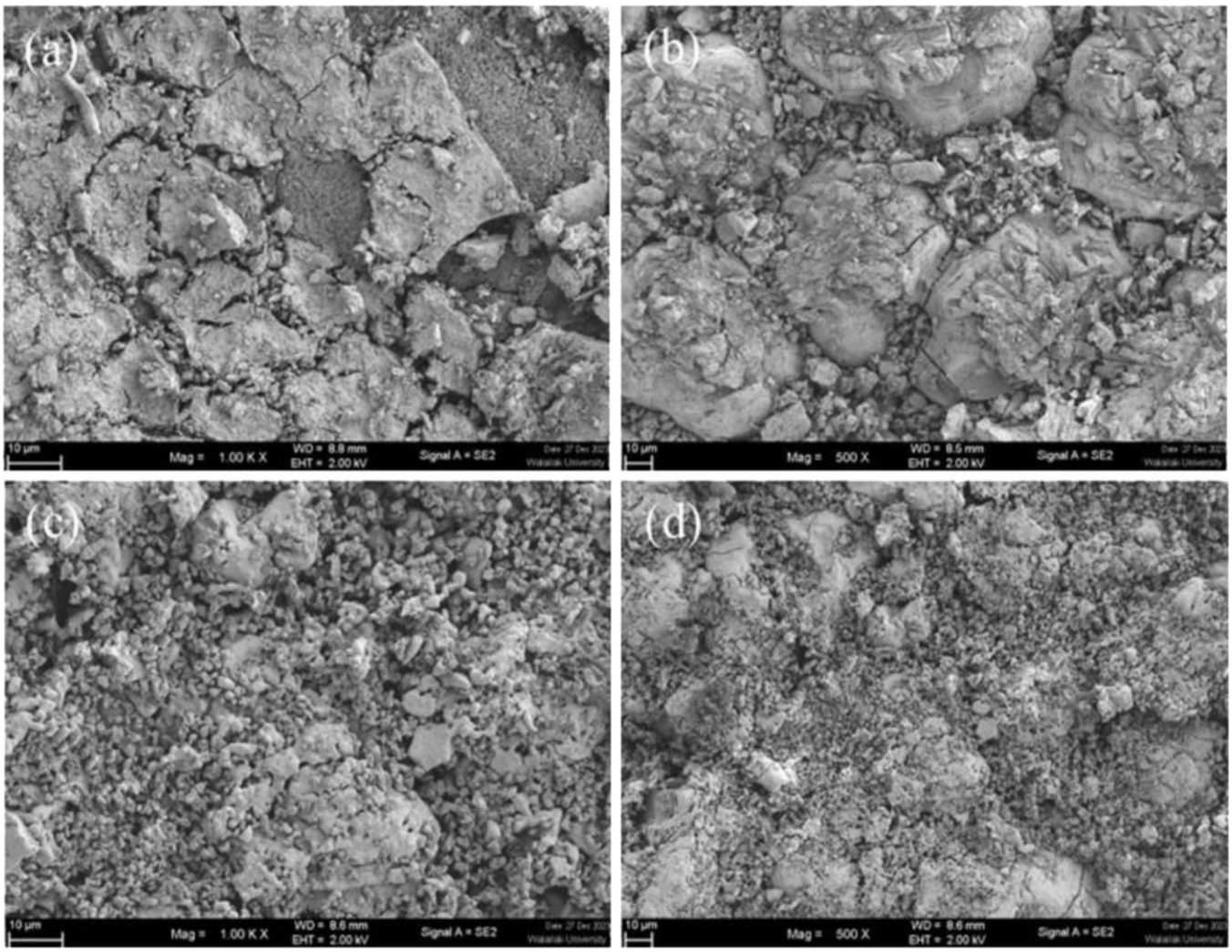

Fig. 2. SEM images of (a) raw eggshell powder and eggshell powders calcined at (b) 400, (c) 600 and (d) 800 ºC

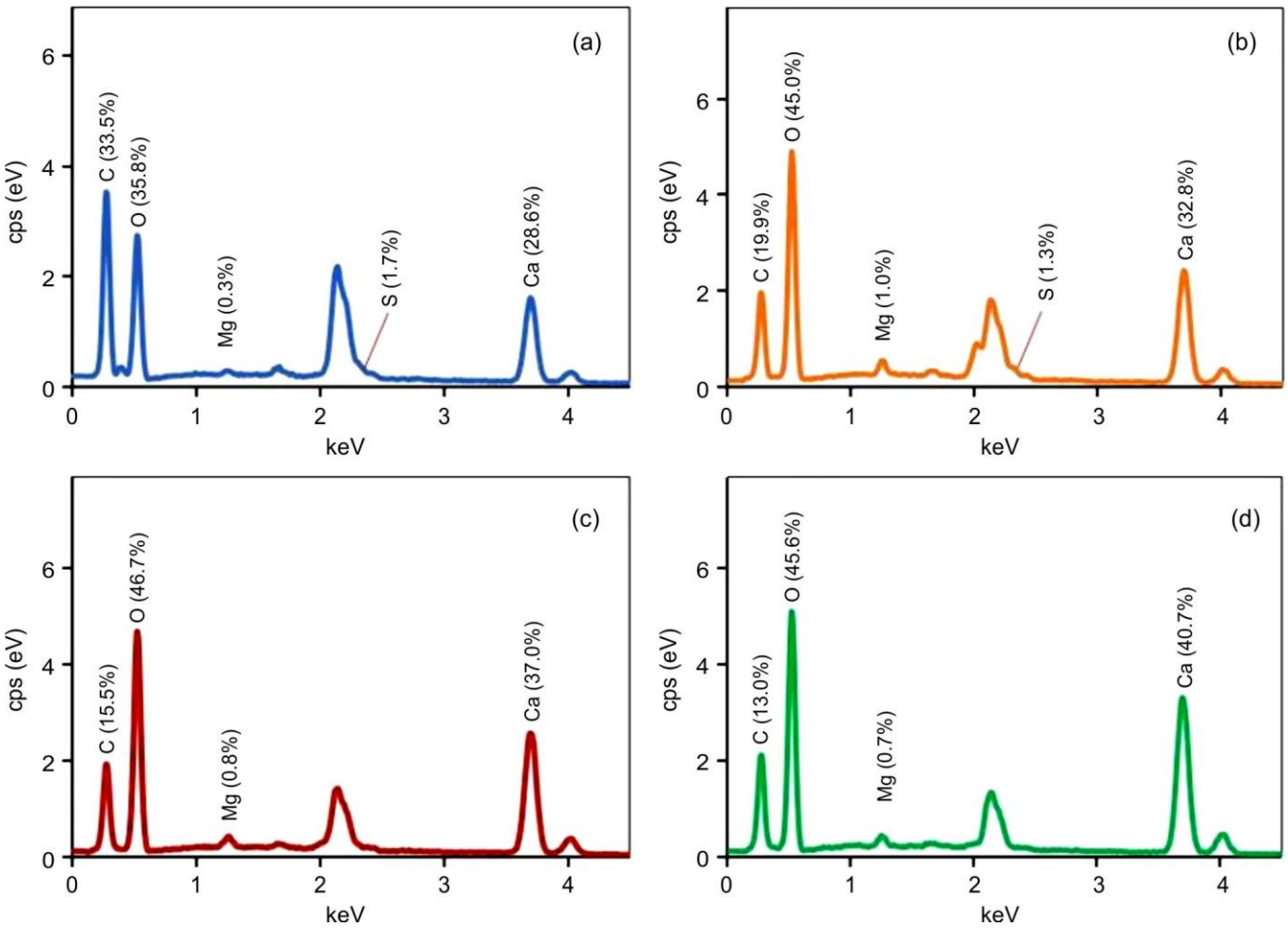

Fig. 3. EDS spectra of (a) raw eggshell powder and eggshell powders calcined at (b) 400, (c) 600 and (d) 800 ºC

static attraction and surface complexation. The SEM images of the same sample reveal particle densification and pore occupied, which can limit the benefit of this compositional change. The EDS results identify 600 ºC as the most favourable calcination temperature, providing a composition that supports efficient adsorption of methylene blue and ofloxacin.

EDS elemental mapping: EDS mapping of calcined eggshell waste at 600 ºC (Fig. 4) reveals uniform distribution of O, C, Mg and Ca across the surface. Dominant O and Ca confirm calcium-based compounds, whereas residual carbon indicates partial carbonate decomposition [19]. Minor Mg disperses evenly within the matrix. This homogeneity ensures abundant, accessible active sites, promoting adsorption *via* electrostatic attraction and surface complexation enhancing the potential of MB/OFX removal.

pH_{pzc} analysis: The pH_{pzc} values of the raw and calcined eggshell materials were determined using the pH drift method, as shown in Fig. 5. The pH_{pzc} values were 4.5, 5.4, 6.6 and 9.9 for the raw eggshell and eggshells calcined at 400, 600 and 800 ºC, respectively. The gradual increase in pH_{pzc} with calcination temperature indicates a significant change in the surface properties of the eggshell materials. The raw eggshell exhibited the lowest pH_{pzc}, due to the predominance of $CaCO_3$ and residual organic components on its surface. Calcination at 400 and 600 ºC increased the pH_{pzc} through the removal of organic matter and partial decomposition of $CaCO_3$, which exposed more basic surface sites. A substantial increase to 9.9 was observed for the sample calcined at 800 ºC, corresponding to the extensive formation of CaO, a strongly basic oxide. The increase in pH_{pzc} suggests enhanced surface basicity after calcination, which can influence adsorption performance. At solution pH values above the pH_{pzc}, the adsorbent surface becomes negatively charged, favouring the adsorption of cationic species, whereas lower pH conditions promote adsorption of anionic species through electrostatic interactions.

Adsorption studies of methylene blue

Effect of initial MB concentration: The effect of initial methylene blue (MB) concentration on adsorption performance using raw and calcined eggshell waste is shown in Fig. 6. As the initial MB concentration increased from 1 to 10 mg/L, the removal efficiency decreased for all samples, whereas the adsorption capacity (q_e) increased. At low MB concentrations (1-2 mg/L), high removal efficiencies were observed, particularly for the calcined samples, with the 600 ºC adsorbent achieving the highest removal efficiency, approximately 90.67%. This behaviour can be attributed to the abundance of available active sites relative to the number of MB molecules, which promotes efficient adsorption [22]. However, as the initial concentration increased, the removal efficiency grad-

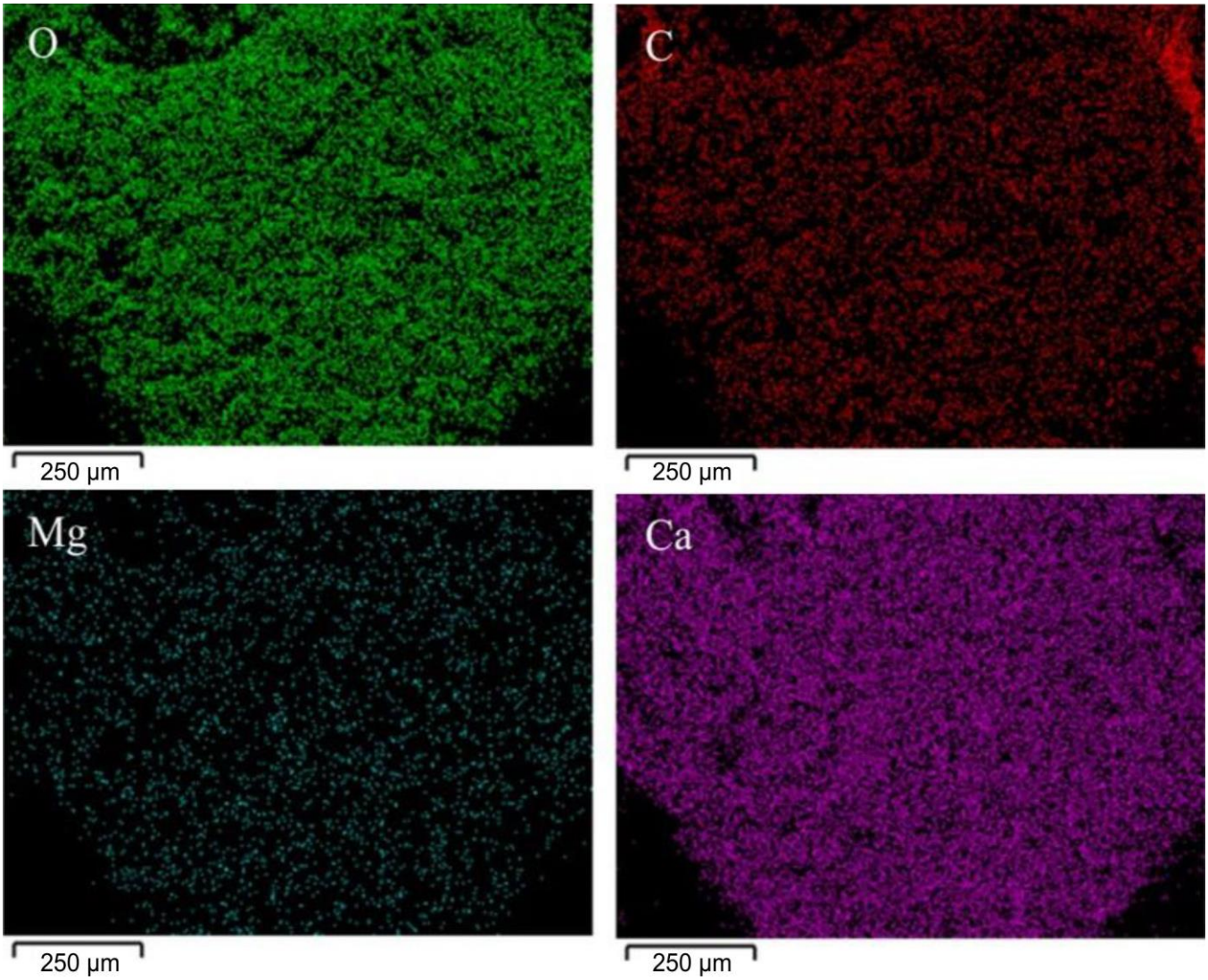

Fig. 4. EDS mapping of the eggshell powder at 600 ºC (a) oxygen, (b) carbon, (c) magnesium and (d) calcium

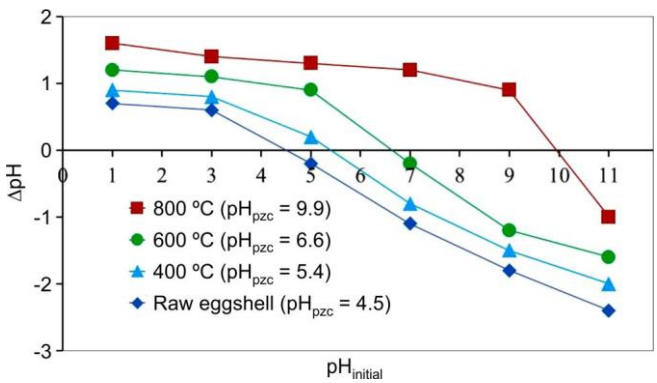

Fig. 5. pH$_{pzc}$ values of raw eggshell powder compare with the calcined eggshell powder at 400 ºC, 600 ºC and 800 ºC

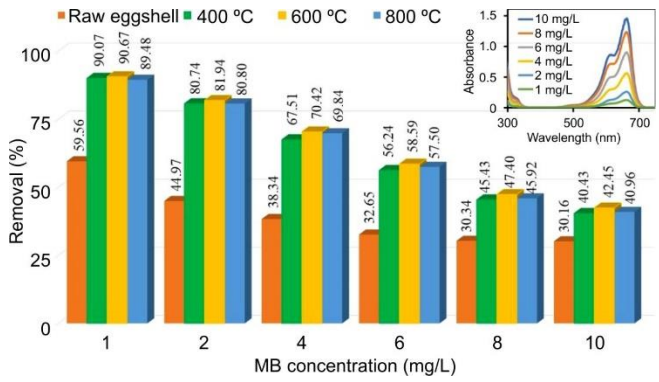

Fig. 6. Effect of initial MB concentration of raw eggshell powder compare with the calcined eggshell powder at 400 ºC, 600 ºC and 800 ºC

ually decreased to about 40-45% at 10 mg/L, due to saturation of the available adsorption sites and increased competition among MB molecules. In contrast, the adsorption capacity increased with increasing MB concentration, indicating that a higher concentration gradient enhances the mass-transfer driving force and promotes diffusion of MB molecules from the bulk solution to the adsorbent surface [23]. Among all samples, the eggshell calcined at 600 ºC consistently exhibited the best performance, followed by those calcined at 400 ºC and 800 ºC, while raw eggshell showed the lowest efficiency. The superior performance at 600 ºC can be attributed to optimal surface characteristics, including enhanced porosity and the

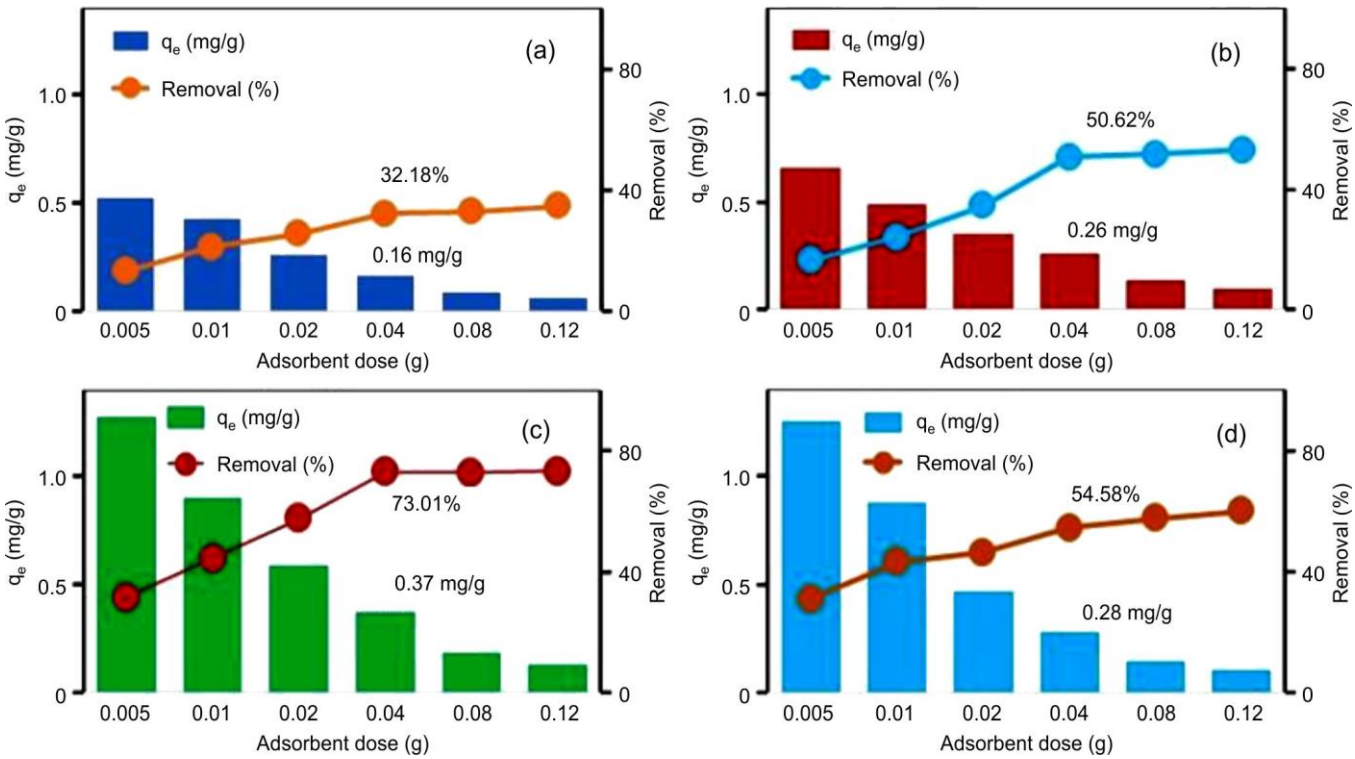

Fig. 7. Effect of adsorbent dose on MB adsorption using (a) raw eggshell and eggshell powders calcined at (b) 400, (c) 600 and (d) 800 ºC

formation of reactive Ca-based sites, as confirmed by SEM and FTIR analyses. Excessive calcination at 800 ºC may have caused pore collapse and reduced the available surface area, resulting in a slight decline in adsorption efficiency. Adsorption performance depended strongly on the initial pollutant concentration and higher removal efficiencies were obtained at lower concentrations. A concentration of 4 mg/L was selected for the subsequent MB adsorption studies due to its reliable UV-Vis response.

Effect of adsorbent dose: The effect of adsorbent dosage on the removal of methylene blue (MB) by raw and calcined eggshell waste is shown in Fig. 7. Increasing the adsorbent dosage from 0.005 to 0.12 g increased the percentage removal of MB for all samples, whereas the adsorption capacity (q_e) decreased. The raw eggshell exhibited a maximum removal efficiency of 32.18% with an adsorption capacity of 0.16 mg/g at an adsorbent dosage of 0.04 g, which can be attributed to its limited surface area and relatively small number of active adsorption sites. Thermal treatment improved the adsorption performance. The sample calcined at 400 ºC achieved a removal efficiency of 50.62%, which may be attributed to the development of surface pores and additional active sites. The highest removal efficiency (73.01%) was obtained for the sample calcined at 600 ºC, with an adsorption capacity of 0.37 mg/g. Partial decomposition of $CaCO_3$ at this temperature increases surface roughness, pore development and the number of accessible adsorption sites. The sample calcined at 800 ºC retained a relatively high removal efficiency (54.58%), although its adsorption capacity was lower than that of the 600 ºC sample. Particle agglomeration and partial pore collapse at higher temperatures may account for this decrease, consistent with the SEM observations [19]. Higher removal efficiencies at lower dosages can be attributed to the greater accessibility of active sites and exposed surface area available for MB adsorption [24]. Increasing the adsorbent dosage lowers the adsorbate-to-adsorbent ratio, leaving a portion of the adsorption sites unoccupied. The results identify eggshell waste calcined at 600 ºC as the most effective adsorbent, while an adsorbent dosage of 0.04 g was selected as the optimum condition for subsequent experiments.

Effect of contact time: The effect of contact time on the adsorption of methylene blue (MB) by raw and calcined eggshell waste is shown in Fig. 8. The adsorption capacity (q_e) increased rapidly during the first 60 min for all samples, followed by a gradual increase until equilibrium was reached at approximately 120 min. The rapid uptake during the initial stage is attributed to the large number of vacant adsorption sites available on the adsorbent surface, which promotes rapid adsorption of MB molecules [22]. Among the tested materials, the eggshell calcined at 600 ºC exhibited the highest

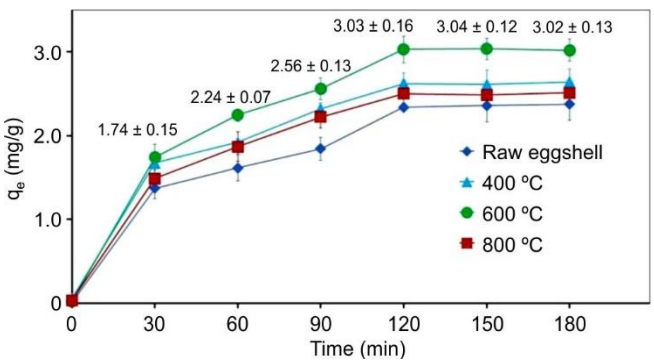

Fig. 8. Effect of contact time on MB adsorption using raw eggshell and eggshell powders calcined at 400, 600 and 800 ºC

TABLE-1
PARAMETERS OF LANGMUIR AND FREUNDLICH ISOTHERMS FOR THE MB ADSORPTION ON THE OBTAINED EGGSHELL POWDERS

Eggshell powder adsorbent	Parameters of Langmuir			Parameters of Freundlich		
	q_m (mg/g)	K_L (L/mg)	R^2	K_F (mg/g)	n	R^2
Raw eggshell	7.65	0.41	0.9953	4.09	3.66	0.9543
Calcined eggshell (400 ºC)	9.11	0.80	0.9871	4.99	5.16	0.9372
Calcined eggshell (600 ºC)	9.95	0.85	0.9922	4.73	5.97	0.9825
Calcined eggshell (800 ºC)	7.44	2.20	0.9978	2.75	3.12	0.9847

adsorption capacity, reaching approximately 3.0 mg/g at equilibrium. This behaviour is associated with the higher porosity and the presence of more reactive calcium-based sites generated during calcination, in agreement with the SEM and FTIR results. The adsorption performance was strongly influenced by both calcination temperature and contact time. The sample calcined at 600 ºC reached the highest adsorption capacity, and an equilibrium time of 120 min was selected for the subsequent adsorption experiments.

Effect of solution pH: The effect of solution pH on the adsorption of methylene blue (MB) by raw and calcined eggshell waste is shown in Fig. 9. The adsorption capacity increased with increasing pH for all adsorbents, although the magnitude of the increase varied with calcination temperature. The sample calcined at 600 ºC exhibited the highest adsorption capacity throughout the investigated pH range, reaching 3.07 mg/g at pH 7 and remaining nearly constant between pH 9 and 11. The sample calcined at 800 ºC exhibited the lowest adsorption capacity under acidic conditions, followed by a sharp increase under alkaline conditions, reaching 3.01 mg/g at pH 11.

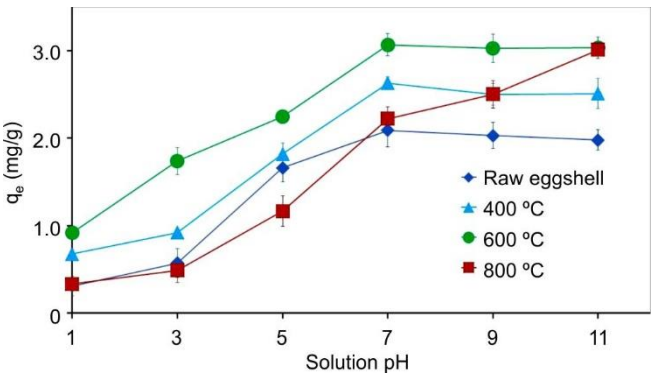

Fig. 9. Effect of solution pH on MB adsorption using raw eggshell and eggshell powders calcined at 400, 600 and 800 ºC

The adsorption behaviour is closely related to the point of zero charge (pH_{PZC}) of the adsorbents. The pH_{PZC} values of the raw eggshell and the samples calcined at 400, 600, and 800 ºC were 4.5, 5.4, 6.6 and 9.9, respectively (Fig. 5). At pH values below the pH_{PZC}, protonation of surface hydroxyl groups gives the adsorbent a positive surface charge, leading to electrostatic repulsion between the surface and the cationic MB molecules. When the solution pH exceeds the pH_{PZC}, deprotonation generates negatively charged surface sites, increasing the electrostatic attraction toward MB molecules.

The sample calcined at 600 ºC exhibited the highest adsorption capacity because its pH_{PZC} (6.6) allows the surface to acquire a negative charge under near-neutral conditions, where MB adsorption is most favorable. The sample calcined at 800 ºC has a much higher pH_{PZC} (9.9), a consequence of CaO formation during calcination. Negative surface sites develop only under strongly alkaline conditions, which explains the lower adsorption at acidic and neutral pH values. The results indicate that electrostatic attraction is the dominant mechanism governing MB adsorption, while calcination at 600 ºC provides the most suitable surface characteristics for efficient adsorption.

Adsorption isotherm of methylene blue (MB): The adsorption behaviour of MB onto raw and calcined eggshell waste was evaluated using the Langmuir and Freundlich isotherm models (Fig. 10) and the corresponding model parameters are listed in Table-1. The Langmuir model gave a better fit to the experimental data than the Freundlich model, supporting monolayer adsorption of MB on the eggshell surface. The Freundlich model also provided an acceptable fit, which may be associated with the heterogeneous nature of the adsorbent surface. The maximum adsorption capacities obtained from the Langmuir model were 7.65, 9.11, 9.95 and 7.44 mg/g for raw eggshell and samples calcined at 400, 600 and 800 ºC, respectively. The highest adsorption capacity of 9.95 mg/g was obtained for the sample calcined at 600 ºC. A comparison of the MB adsorption capacities of different adsorbents is provided in Table-2. The adsorption capacity of the calcined eggshell waste was comparable to those reported for several other low-cost adsorbents, supporting its potential for the removal o MB from aqueous solutions.

TABLE-2
COMPARATIVE DATA OF DIFFERENT ADSORBENTS USED FOR METHYLENE BLUE (MB) ADSORPTION

Adsorbent	q_m (mg/g)	Ref.
Al Haji plant	5.24	[25]
Rice husk-activated carbon	9.73	[26]
Cashew nut shell	5.31	[27]
Canola residues	7.11	[28]
Raw eggshell	7.65	This work
Calcined eggshell (400 ºC)	9.11	This work
Calcined eggshell (600 ºC)	9.95	This work
Calcined eggshell (800 ºC)	7.44	This work

Ofloxacin antibiotic removal studies

Effect of ofloxacin concentration: The effect of the initial ofloxacin (OFX) concentration on the adsorption performance of raw and calcined eggshell waste is shown in Fig. 11a-d. Increasing the initial OFX concentration from 1 to 10

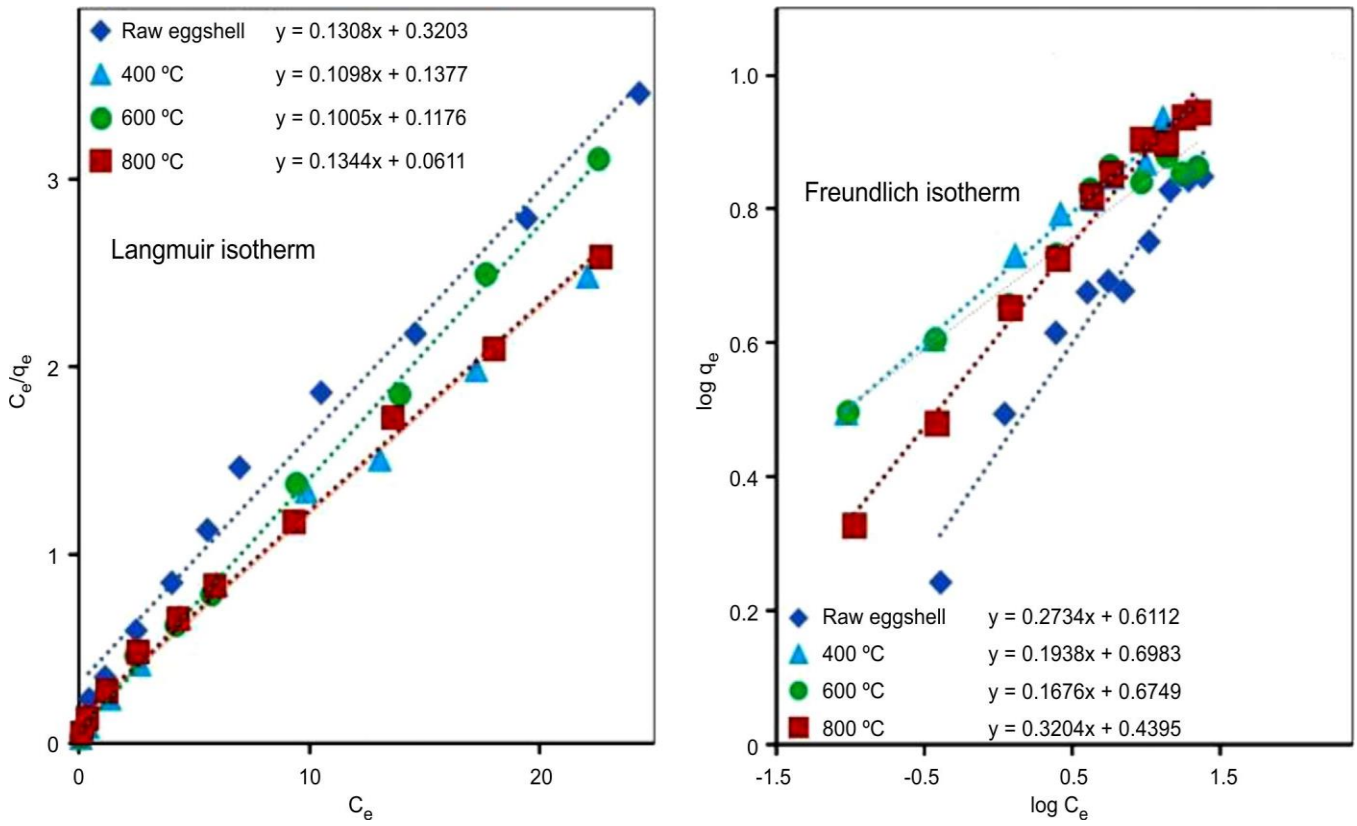

Fig. 10. Langmuir and Freundlich isotherms for OFX adsorption onto raw eggshell and eggshell powders calcined at 400, 600 and 800 ºC

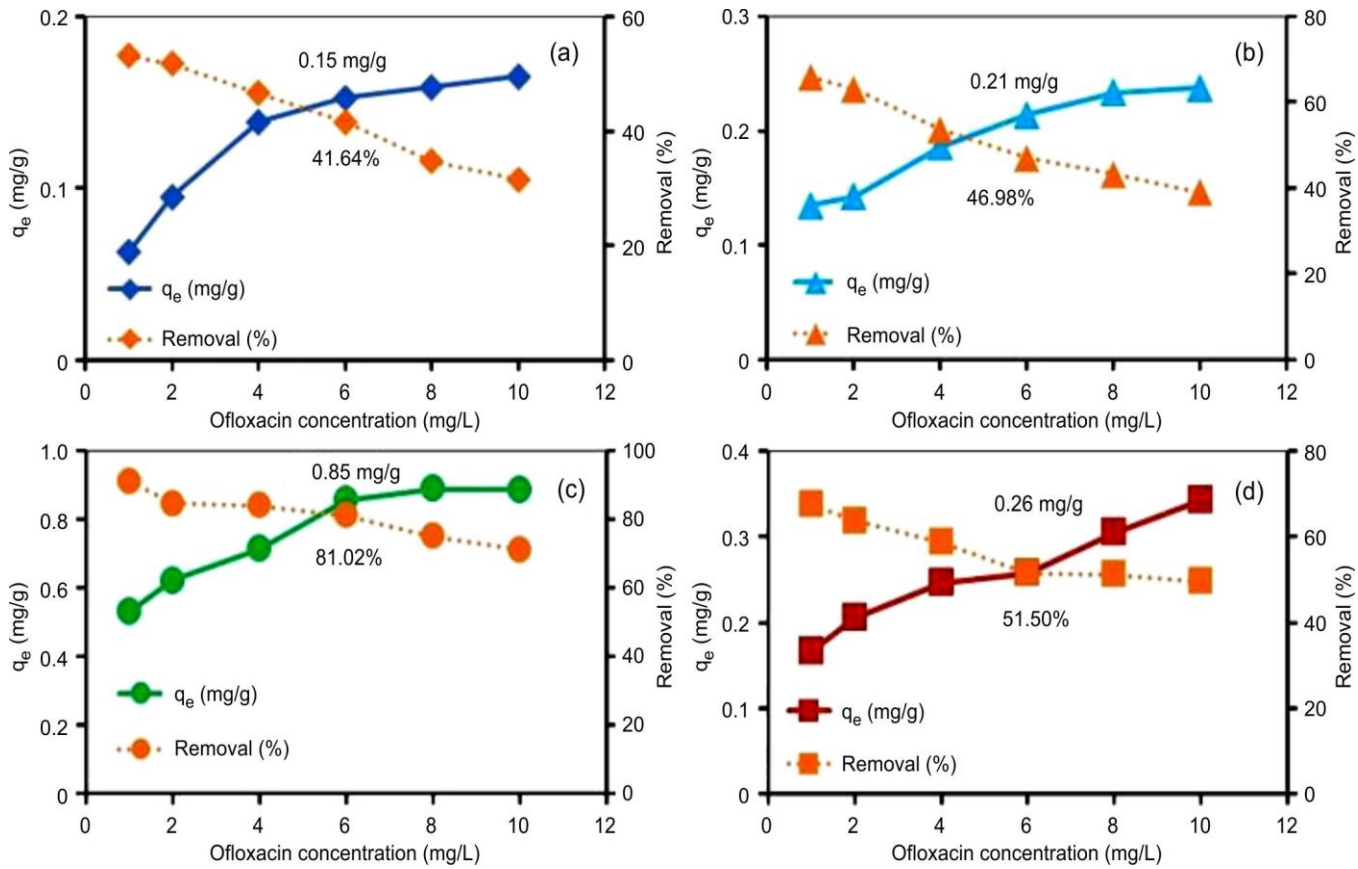

Fig. 11. Effect of initial OFX concentration on adsorption using (a) raw eggshell and eggshell powders calcined at (b) 400, (c) 600 and (d) 800 ºC

mg/L increased the adsorption capacity (q_e) of all samples, whereas the removal efficiency decreased.

The high removal efficiencies were obtained at low OFX concentrations (1-2 mg/L), where the number of available adsorption sites exceeded the number of OFX molecules. Increasing the initial concentration gradually reduced the removal efficiency due to progressive occupation of the available adsorption sites and better competition among OFX molecules. The adsorption capacity followed the opposite trend, reaching approximately 0.15, 0.21, 0.85 and 0.26 mg/g for raw eggshell and samples calcined at 400, 600 and 800 ºC, respectively. The higher concentration gradient at elevated OFX concentrations increases the mass transfer driving force and facilitates diffusion of OFX molecules to the adsorbent surface [29].

The sample calcined at 600 ºC exhibited the highest adsorption capacity and removal efficiency, which can be attributed to its well-developed pore structure and higher number of reactive calcium-based adsorption sites. The raw eggshell exhibited the lowest adsorption performance owing to its limited surface area and fewer active sites. Calcination at 800 ºC reduced the adsorption capacity, which may be associated with particle densification and partial loss of porosity at higher temperatures. The adsorption performance depended strongly on the initial OFX concentration through the combined effects of adsorption-site availability and mass transfer [29]. An initial OFX concentration of 6 mg/L was selected as the optimum condition for the subsequent adsorption experiments.

Effect of adsorbent dose: The effect of adsorbent dosage on the removal of ofloxacin (OFX) by raw and calcined eggshell waste is shown in Fig. 12a-d. Increasing the adsorbent dosage from 0.005 to 0.12 g increased the removal efficiency of OFX for all samples, whereas the adsorption capacity (q_e) decreased. The raw eggshell (Fig. 12a) achieved a maximum removal efficiency of 56.67% with an adsorption capacity of 0.16 mg/g at an adsorbent dosage of 0.04 g. The relatively low adsorption performance is associated with its limited surface area and fewer available adsorption sites. Thermal treatment improved the adsorption performance. The sample calcined at 400 ºC (Fig. 12b) reached a removal efficiency of 64.33%, while calcination at 600 ºC (Fig. 12c) increased the removal efficiency to 85.34% with an adsorption capacity of 0.24 mg/g. The higher adsorption performance is attributed to higher pore development, increased surface area and a larger number of accessible adsorption sites generated during calcination [29].

The sample calcined at 800 ºC (Fig. 12d) retained a removal efficiency of 66.74%, although its adsorption capacity was lower than that of the sample calcined at 600 ºC. Particle agglomeration and partial pore collapse at higher calcination temperatures may reduce the effective surface area available for adsorption. The decrease in q_e with increasing adsorbent dosage is associated with particle aggregation and overlapping of adsorption sites, which limits their accessibility. A higher adsorbent dosage also lowers the adsorbate-to-adsorbent ratio, leaving part of the available surface unoccupied. An adsorbent dosage of 0.04 g was selected as the optimum condition for the subsequent OFX adsorption experiments.

Effect of contact time: The effect of contact time on the removal of ofloxacin (OFX) by raw and calcined eggshell waste is shown in Fig. 13. The removal efficiency increased rapidly during the first 60 min for all samples and gradually

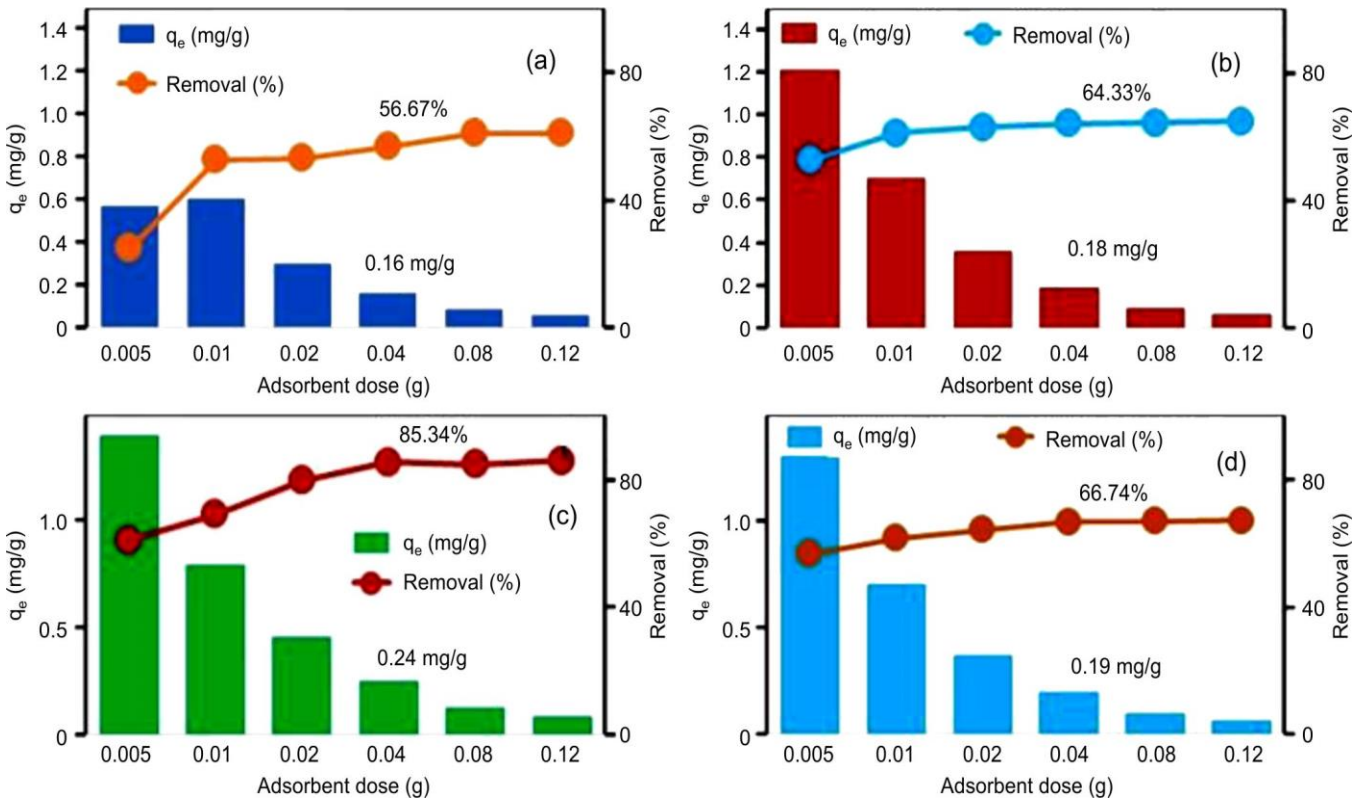

Fig. 12. Effect of adsorption dose of raw eggshell and eggshell powders calcined at 400, 600 and 800 ºC for ofloxacin adsorption

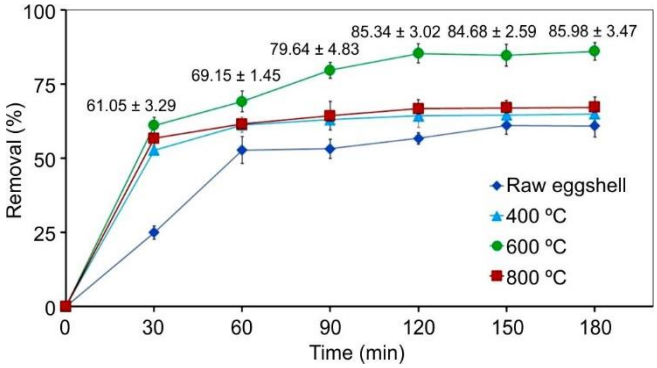

Fig. 13. Effect of contact time on OFX adsorption using raw eggshell and eggshell powders calcined at 400, 600 and 800 °C

reached equilibrium within 120-150 min. The rapid adsorption during the initial stage is attributed to the large number of vacant adsorption sites available on the adsorbent surface, which promotes the adsorption of OFX molecules [30].

The sample calcined at 600 °C exhibited the highest removal efficiency, reaching approximately 85% at equilibrium. The improved adsorption performance is associated with higher porosity and a higher number of reactive calcium based sites generated during calcination, consistent with the SEM and FTIR results. The samples calcined at 400 and 800 °C exhibited intermediate adsorption performance, whereas the raw eggshell showed the lowest removal efficiency owing to its compact structure and limited number of accessible adsorption sites. The adsorption rate slowed after 60 min as the available adsorption sites became progressively occupied and mass transfer resistance increased. A nearly constant removal efficiency after 120 min indicates that adsorption equilibrium had been established, with adsorption and desorption occurring at comparable rates. The adsorption process is likely controlled by both surface adsorption and intraparticle diffusion. An equilibrium time of 120 min was selected as the optimum condition for the subsequent OFX adsorption experiments.

Effect of solution pH: The effect of solution pH on the adsorption of ofloxacin (OFX) by raw and calcined eggshell waste is shown in Fig. 14. The adsorption capacity increased with increasing pH, reached a maximum at pH 7 and decreased under alkaline conditions. The sample calcined at 600 °C exhibited the highest adsorption capacity (0.24 mg/g) at pH 7, followed by the samples calcined at 800 °C (0.19 mg/g) and

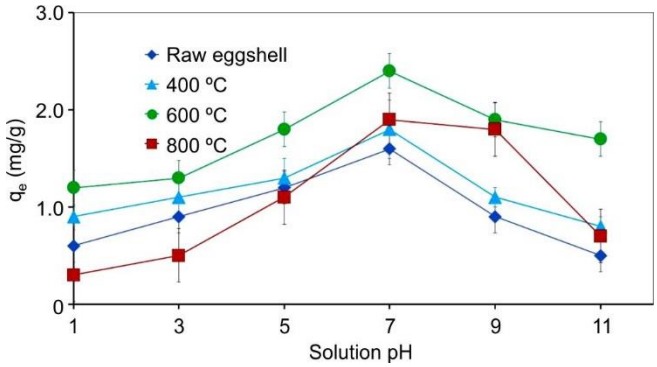

Fig. 14. Effect of solution pH on OFX adsorption using raw eggshell and eggshell powders calcined at 400, 600 and 800 °C

400 °C (0.18 mg/g), while the raw eggshell exhibited the lowest adsorption capacity (0.16 mg/g).

The adsorption behavior depends on both the pH_{PZC} of the adsorbents and the pH-dependent speciation of OFX. The pH_{PZC} values of the raw eggshell and the samples calcined at 400, 600 and 800 °C were 4.5, 5.4, 6.6 and 9.9, respectively. At acidic pH, the adsorbent surfaces carry a positive charge, and OFX is predominantly present in its cationic form. The electrostatic repulsion between the adsorbent and OFX limits adsorption under these conditions. Near neutral pH, OFX exists mainly as a zwitterion, allowing electrostatic interactions, hydrogen bonding and surface complexation with calcium-containing adsorption sites. These interactions favour adsorption and account for the highest adsorption capacity observed at pH 7.

Under alkaline conditions, OFX is present mainly in its anionic form and the adsorption capacity decreases as the surfaces of the raw, 400 °C and 600 °C samples become negatively charged. The sample calcined at 800 °C retains a positive surface charge below its pH_{PZC} (9.9), yet its adsorption capacity still declined at pH 11. This behaviour suggests that electrostatic attraction alone cannot account for OFX adsorption and that other interactions contribute to the adsorption process. The sample calcined at 600 °C provided the most suitable surface characteristics for OFX adsorption.

Adsorption isotherm of ofloxacin: The adsorption behaviour of ofloxacin (OFX) onto raw and calcined eggshell waste was evaluated using the Langmuir and Freundlich isotherm models (Fig. 15) and the corresponding parameters are shown in Table-3. The Langmuir model provided a better fit to the experimental data, supporting monolayer adsorption of OFX on the eggshell surface. The sample calcined at 600 °C exhibited the lowest Langmuir slope and a favourable intercept, corresponding to the highest adsorption capacity and the strongest affinity for OFX molecules. The raw eggshell exhibited the lowest adsorption performance, which can be attributed to its limited surface area and lower number of available adsorption sites.

The Freundlich model also described the experimental data reasonably well, which is consistent with the heterogeneous nature of the adsorbent surface. The maximum adsorption capacities obtained from the Langmuir model were 0.19, 0.26, 0.93 and 0.36 mg/g for raw eggshell and the samples calcined at 400, 600 and 800 °C, respectively. The highest adsorption capacity (0.93 mg/g) was obtained for the sample calcined at 600 °C. A comparison of OFX adsorption capacities reported for different adsorbents is shown in Table-4. The adsorption capacity of eggshell waste calcined at 600 °C is comparable with those of several low-cost adsorbents, supporting its potential for OFX removal from aqueous solutions.

Kinetic studies: The adsorption kinetics of methylene blue (MB) onto eggshell waste calcined at 600 °C were analyzed using the pseudo-first-order, pseudo-second-order and intraparticle diffusion models. The corresponding plots and kinetic parameters are shown in Fig. 16. The pseudo-first-order model gave a correlation coefficient (R^2) of 0.8380 with a calculated equilibrium adsorption capacity (q_e) of 2.70 mg/g, which was lower than the experimental value (q_e = 3.44 mg/g). The pseudo-second-order model gave a lower correlation coefficient (R^2

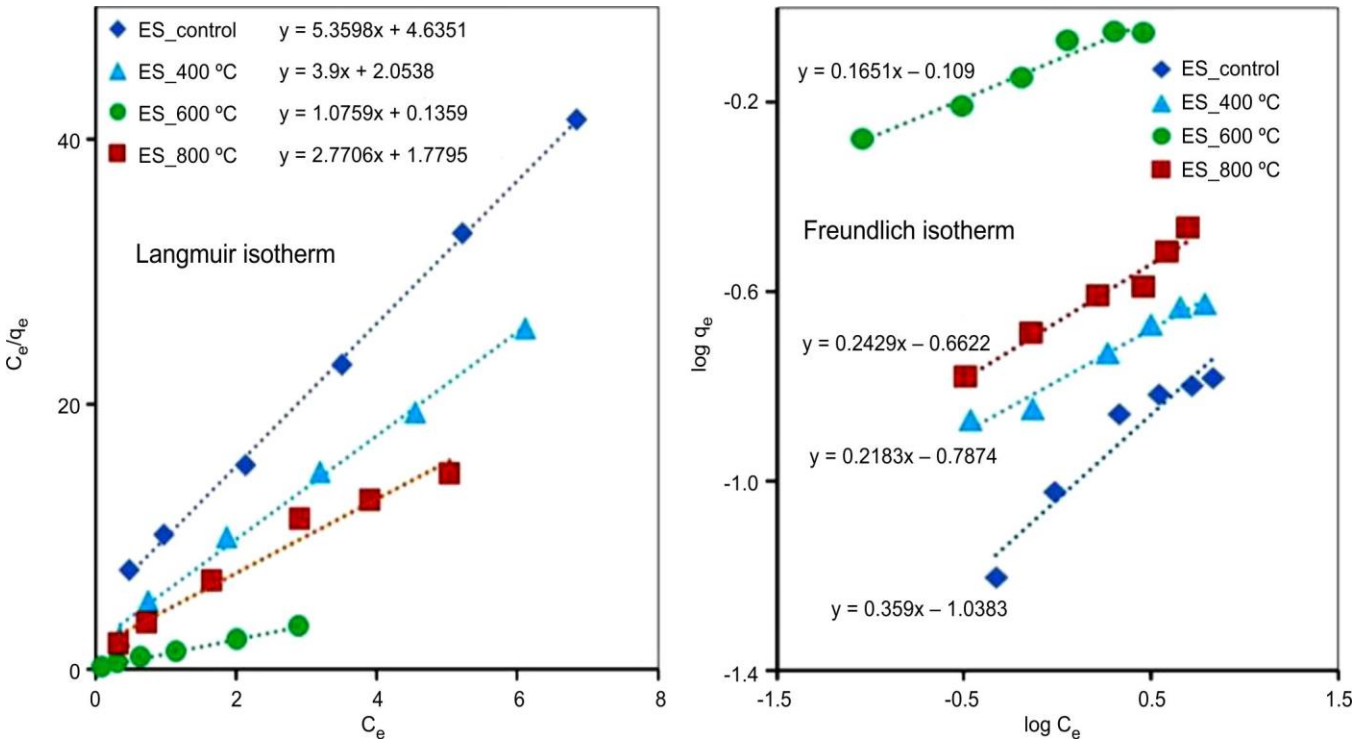

Fig. 15. Langmuir and Freundlich isotherms for OFX adsorption onto eggshell powders calcined at 400, 600 and 800 ºC

TABLE-3
PARAMETERS OF LANGMUIR AND FREUNDLICH ISOTHERMS FOR THE OFX ADSORPTION ON THE OBTAINED EGGSHELL POWDERS

Eggshell powder adsorbent	Parameters of Langmuir			Parameters of Freundlich		
	q_m (mg/g)	K_L (L/mg)	R^2	K_F (mg/g)	n	R^2
Raw eggshell	0.19	1.16	0.9989	2.29	2.79	0.9311
Calcined eggshell (400 ºC)	0.26	1.90	0.9959	1.65	4.58	0.9723
Calcined eggshell (600 ºC)	0.93	1.00	0.9981	1.46	6.06	0.9641
Calcined eggshell (800 ºC)	0.36	1.56	0.9710	1.75	4.12	0.9618

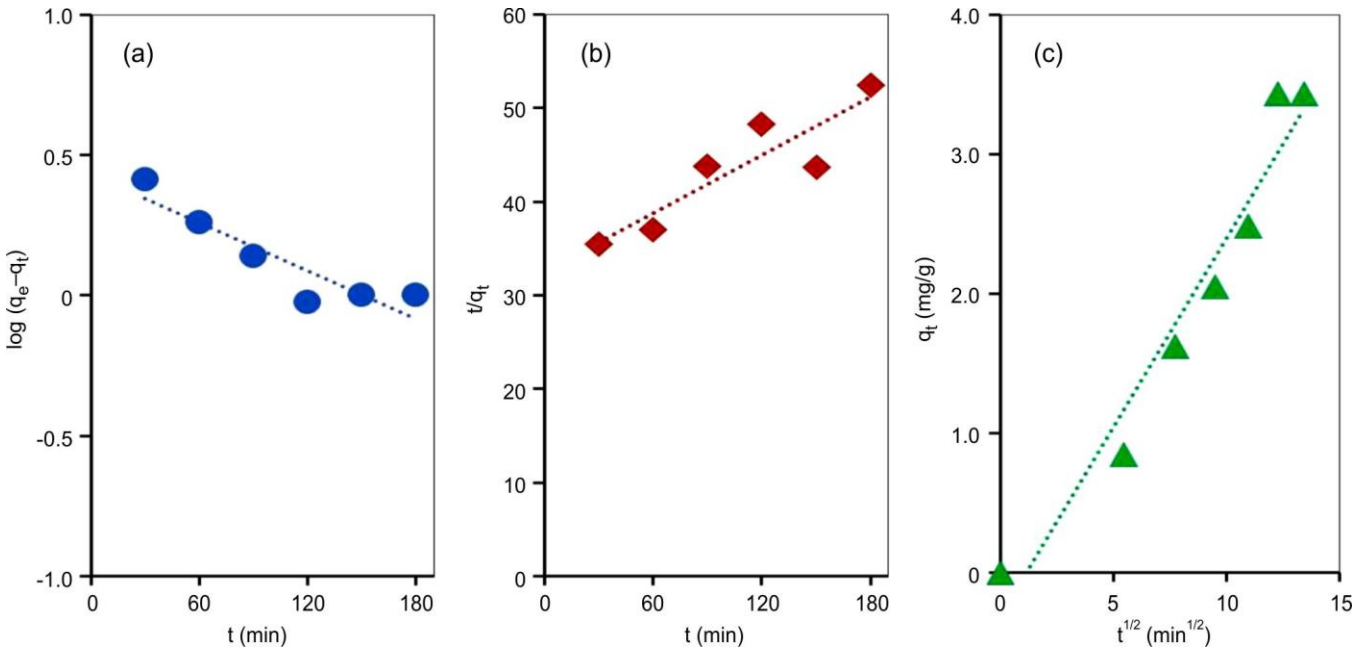

Fig. 16. Kinetic plots of (a) pseudo-first order, (b) pseudo-second order and (c) intra-particle diffusion of the 600 ºC calcined eggshell for MB adsorption at 303 K

TABLE-4
COMPARATIVE ADSORPTION PERFORMANCE OF DIFFERENT ADSORBENTS FOR OFX REMOVAL

Adsorbent	q_m (mg/g)	Ref.
Polystyrene (PS)	0.02933 (29.33 µg/g)	[31]
Polyvinyl chloride (PVC)	0.03047 (30.47 µg/g)	[31]
Raw eggshell	0.19	This work
Calcined eggshell (400 ºC)	0.26	This work
Calcined eggshell (600 ºC)	0.93	This work
Calcined eggshell (800 ºC)	0.36	This work

= 0.8142) and overestimated the equilibrium adsorption capacity (9.62 mg/g). Neither model adequately described the adsorption kinetics of MB under the experimental conditions (Table-5).

The intraparticle diffusion model exhibited the highest correlation coefficient (R^2 = 0.9494), suggesting that pore diffusion contributed significantly to the adsorption process. The positive intercept (C = 0.31 mg/g) means that the regression line did not pass through the origin, suggesting that intraparticle diffusion was not the only rate-controlling step. MB adsorption likely involved film diffusion, surface adsorption and diffusion within the pores of the calcined eggshell. This interpretation is consistent with the porous morphology observed by SEM. A multistep diffusion process provides a better description of the adsorption kinetics than a single kinetic model.

The adsorption kinetics of OFX onto eggshell waste calcined at 600 ºC were analyzed using the same kinetic models, and the results are shown in Fig. 17. The pseudo-first-order model gave a calculated equilibrium adsorption capacity of 0.45 mg/g, close to the experimental value (q_e = 0.49 mg/g), with a correlation coefficient (R^2) of 0.9016. The pseudo-second-order model provided the best fit, with the highest correlation coefficient (R^2 = 0.9922) and a calculated equilibrium adsorption capacity (0.51 mg/g) that closely matched the experimental value (Table-6).

The close agreement between the experimental and calculated adsorption capacities suggests that OFX adsorption is dominated by chemisorption. Calcium-containing surface species and hydroxyl groups formed during calcination can interact with OFX through hydrogen bonding, surface complexation and electrostatic attraction. The intraparticle diffusion model gave a lower correlation coefficient (R^2 = 0.8899). Its positive intercept (C = 0.08 mg/g) indicates that pore diffusion alone does not control the adsorption rate. Film diffusion, surface adsorption and intraparticle diffusion all contribute to the adsorption process, with surface adsorption playing the major role.

Thermodynamic studies: The thermodynamic parameters for the adsorption of MB and OFX onto eggshell waste calcined at 600 ºC are shown in Table-7. The standard Gibbs free energy (ΔGº) values remained negative throughout the investigated temperature range for both adsorbates, confirmed the spontaneous nature of adsorption. As the temperature increased, the ΔGº values became more negative, making adsorption thermodynamically more favorable. For MB, the ΔGº values ranged from -1.43 to -2.53 kJ/mol and the positive standard enthalpy change (ΔHº = 9.16 kJ/mol) identifies the process as endothermic. The corresponding ΔGº values for OFX ranged from -0.45 to -2.22 kJ/mol. Its higher positive enthalpy change (ΔHº = 16.39 kJ/mol) indicates that OFX adsorption required a higher energy input than MB adsorption.

The positive standard entropy changes for MB (0.04 kJ/mol K) and OFX (0.06 kJ/mol K) are consistent with increased randomness at the adsorbent–solution interface during adsorption. This increase may arise from the displacement of water molecules from the adsorbent surface and the rearrangement of adsorbed molecules. The relatively low ΔHº values (< 40 kJ/mol) are the characteristic of physisorption, although electrostatic attraction, hydrogen bonding and surface complexation are likely to contribute to the adsorption process. The coefficients of determination obtained from the

TABLE-5
KINETIC PARAMETERS OF MB ADSORPTION USING THE 600 ºC CALCINED EGGSHELL AT 303 K

$q_{e,exp}$ (mg/g)	Pseudo-first order		Pseudo-second order		Intra-particle diffusion	
3.44	q_e (mg/g)	2.70	q_e (mg/g)	9.62	C (mg/g)	0.31
	k_1 (min^{-1})	0.01	k_2 (g/mg min)	0.0003	k_{id} (mg/g $min^{1/2}$)	0.27
	R^2	0.8380	R^2	0.8142	R^2	0.9494

TABLE-6
KINETIC PARAMETERS OF OFLOXACIN ADSORPTION USING THE 600 ºC CALCINED EGGSHELL AT 303 K

$q_{e,exp}$ (mg/g)	Pseudo-first order		Pseudo-second order		Intra-particle diffusion	
0.49	q_e (mg/g)	0.45	q_e (mg/g)	0.51	C (mg/g)	0.08
	k_1 (min^{-1})	0.03	k_2 (g/mg min)	4.72	k_{id} (mg/g $min^{1/2}$)	0.04
	R^2	0.9016	R^2	0.9922	R^2	0.8899

TABLE-7
THERMODYNAMIC PARAMETERS OF MB AND OFX ADSORPTION USING THE 600 ºC CALCINED EGGSHELL ADSORBENT

Adsorbate	ΔGº (kJ/mol)				ΔHº (kJ/mol)	ΔSº (kJ/mol·K)
	288.15 K	303.15 K	318.15 K	R^2		
MB	-1.43	-2.05	-2.53	0.9932	9.16	0.04
OFX	-0.45	-0.80	-2.22	0.8728	16.39	0.06

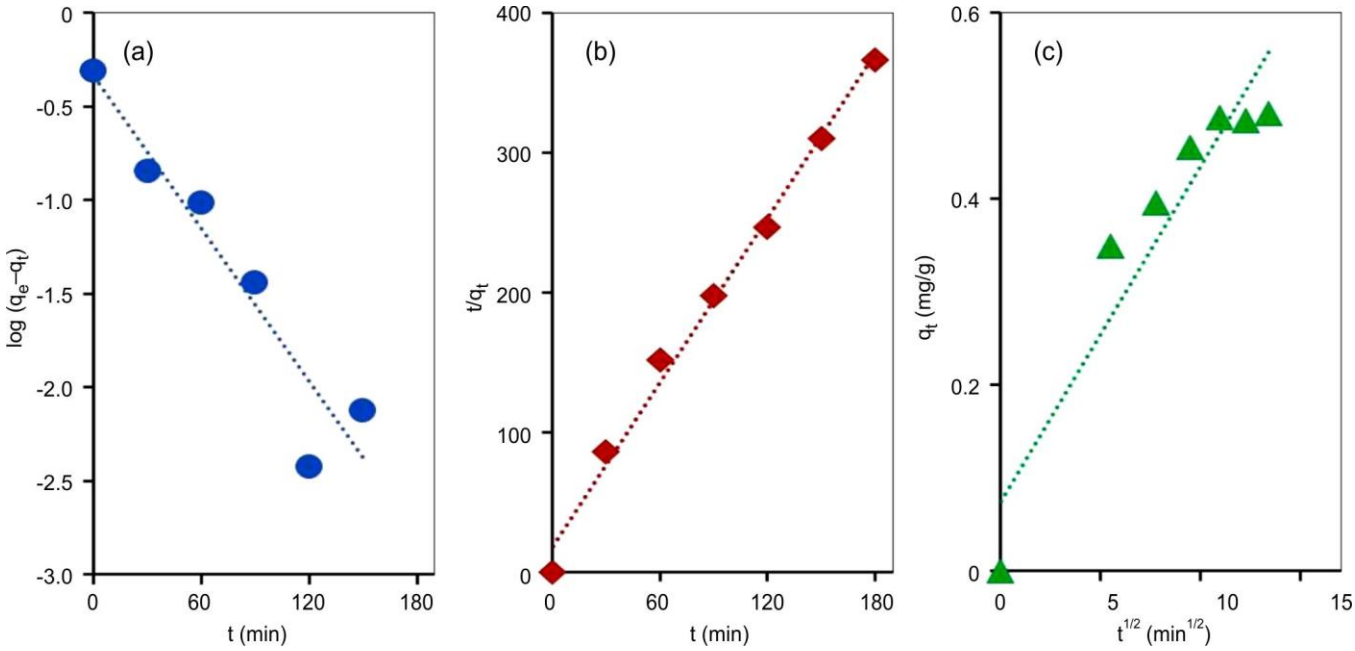

Fig. 17. Kinetic plots of (a) pseudo-first order, (b) pseudo-second order and (c) intra-particle diffusion of the 600 ºC calcined eggshell for ofloxacin adsorption at 303 K

van't Hoff plots were 0.9932 for MB and 0.8728 for OFX, which shows that the experimental data were adequately described by the van't Hoff model.

Reusability: The reusability of eggshell waste calcined at 600 ºC for the removal of MB and OFX was evaluated over five consecutive adsorption-desorption cycles and the results are shown in Fig. 18. The adsorbent retained satisfactory adsorption performance during repeated use, although the removal efficiency gradually decreased with successive regeneration cycles. For MB, the removal efficiency decreased from 73.32 ± 3.25% in the first cycle to 50.04 ± 1.98% after the fifth cycle. The removal efficiency of OFX decreased from 85.98 ± 2.54% to 50.21 ± 3.49% over the same period. The loss in adsorption performance can be attributed to incomplete desorption of MB and OFX molecules, leaving part of the adsorption sites occupied after each regeneration cycle. Repeated regeneration may also cause slight structural changes, pore blockage or partial loss of surface functional groups, reducing the number of accessible adsorption sites.

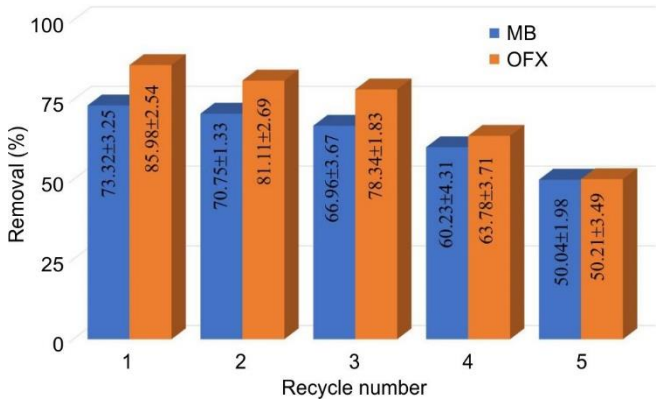

Fig. 18. Reusability of the 600 ºC calcined eggshell adsorbent for MB and OFX removal

OFX exhibited a higher initial removal efficiency than MB, which may be related to additional interactions between OFX molecules and the adsorbent surface, such as hydrogen bonding and surface complexation, together with electrostatic attraction. These interactions can make desorption less effective, leading to a gradual reduction in adsorption performance during repeated use. The adsorbent retained approximately 50% removal efficiency for both pollutants after five adsorption-desorption cycles, which reflects good structural stability and satisfactory reusability.

Conclusion

This study investigated the use of eggshell waste as an adsorbent for the removal of methylene blue (MB) and ofloxacin (OFX) from aqueous solutions. The optimum adsorption conditions were an adsorbent dosage of 0.04 g, a contact time of 120 min, an initial MB concentration of 4 mg/L and an initial OFX concentration of 6 mg/L. Under these conditions, the maximum removal efficiencies reached 73.01% for MB and 85.34% for OFX, with corresponding maximum adsorption capacities of 9.95 and 0.93 mg/g, respectively. Kinetic analysis showed that MB adsorption followed a multistep diffusion process, whereas OFX adsorption was best described by the pseudo-second-order kinetic model. Thermodynamic studies showed that the adsorption of both pollutants was spontaneous and endothermic. The adsorbent retained more than 50% of its MB and OFX removal efficiencies after five adsorption-desorption cycles, which reflects its good reusability. Eggshell waste calcined at 600 ºC offers a low-cost, environmentally friendly, and reusable adsorbent with good potential for the removal of MB and OFX from wastewater.

ACKNOWLEDGEMENTS

This work was funded by Nakhon Si Thammarat Rajabhat University, the Ministry of Higher Education, Science, Research and Innovation. The authors are grateful for providing the equipment support offered by the Center of Excellence in Nanomaterials Chemistry, Nakhon Si Thammarat Rajabhat University, Thailand.

CONFLICT OF INTEREST

The authors declare that there is no conflict of interests regarding the publication of this article.

DECLARATION OF AI-ASSISTED TECHNOLOGIES

During the preparation of this manuscript, the authors used an AI-assisted tool(s) to improve the language and no data, results or scientific conclusions were generated by AI. All analyses, interpretations and conclusions are the authors' own. The authors reviewed and edited the content and take full responsibility for the published work.

REFERENCES

1. R. Al-Tohamy, S.S. Ali, F. Li, K.M. Okasha, Y.A.G. Mahmoud, T. Elsamahy, H. Jiao, Y. Fu and J. Sun, *Ecotoxicol. Environ. Saf.*, **231**, 113160 (2022); https://doi.org/10.1016/j.ecoenv.2021.113160
2. Z.M. Hanafiah, W.H.M.Wan Mohtar, K.N.A. Maulud, W.A.A.Q.Imad Wan-Mohtar, M.N. Ebrahim, T.S.B. Abd Manan, A. Indarto, H.A. Afan and Z.M. Yaseen, *Emerg. Contam.*, **11**, 100585 (2025); https://doi.org/10.1016/j.emcon.2025.100585
3. M.I. Din, R. Khalid, J. Najeeb and Z. Hussain, *J. Clean. Prod.*, **298**, 126567 (2021); https://doi.org/10.1016/j.jclepro.2021.126567
4. V.A. Thai, V.D. Dang, N.T. Thuy, B. Pandit, T.K.Q. Vo and A.P. Khedulkar, *J. Clean. Prod.*, **418**, 137762 (2023); https://doi.org/10.1016/j.jclepro.2023.137762
5. Q. Feng, K. Guo, B. Liu, C. Wang, B. Yan, Q. Yue, Y. Gao and B. Gao, *J. Clean. Prod.*, **514**, 145825 (2025); https://doi.org/10.1016/j.jclepro.2025.145825
6. Y. Yang, X. Zeng, Z. Zeng, L. Wang, P. Zhu, L. Tang and L. Zhu, *Sep. Purif. Technol.*, **380**, 135308 (2026); https://doi.org/10.1016/j.seppur.2025.135308
7. D. Iqbal, R. Ullah, R. Zhao, Y. Dou, D. Yan and X. Ning, *Sep. Purif. Technol.*, **339**, 126677 (2024); https://doi.org/10.1016/j.seppur.2024.126677
8. J. Sánchez-SanMartín, S.L. Márquez, G Espina, R. Cortés-Antiquera, J. Sun and J.M. Blamey, *Biomolecules* **14**, 369 (2024); https://doi.org/10.3390/biom14030369
9. Momina and K. Ahmad, *J. Clean. Prod.*, **388**, 136014 (2023); https://doi.org/10.1016/j.jclepro.2023.136014
10. S.E. Meziani, H. Agnaou, H.E. Haddaj, W. Boumya, N. Barka and A. Elhalil, *Clean Chem. Eng.*, **12**, 100210 (2025); https://doi.org/10.1016/j.clce.2025.100210
11. Z.T. Chong, L.S. Soh and W.F. Yong, *Results Eng.*, **17**, 100960 (2023); https://doi.org/10.1016/j.rineng.2023.100960
12. M.G. Rinaudo, S.E. Collins and M.R. Morales, *Eng. Proc.*, **67**, 36 (2024); https://doi.org/10.3390/engproc2024067036
13. A. Manyatshe and L.L. Sibali, *Heliyon*, **11**, e42278 (2025); https://doi.org/10.1016/j.heliyon.2025.e42278
14. B.B. Kargule, M. Al-Asadi, S. Al-Anssari, H.S.S. Aljibori, H.T. Hamzah, K.T. Tastambek, T.A. Abdullah and O.I. Abdullah, *ASEAN J. Sci. Eng.*, **5**, 369 (2025); http://ejournal.upi.edu/index.php/AJSE/
15. A. Murcia-Salvador, J.A. Pellicer, M.I. Rodríguez-López, V.M. Gómez-López, E. Núñez-Delicado and J.A. Gabaldón, *Materials*, **13**, 1262 (2020); https://doi.org/10.3390/ma1306126
16. W.I. Mortada, M.M. Ghaith, N.E. Khedr, M.I. Ellethy, A.W. Mohsen and A.L. Shafik, *Environ. Sci. Pollut. Res.*, **31**, 42330 (2024); https://doi.org/10.1007/s11356-024-33860-3
17. K. Kaliannan and S. Kaliannan, *Global NEST J.*, **27**, 07639 (2025); https://doi.org/10.30955/gnj.07639
18. M.S. Tizo, L.A.V. Blanco, A.C.Q. Cagas, B.R.B.D. Cruz, J.C. Encoy, J.V. Gunting, R.O. Arazo and V.I.F. Mabayo, *Sustain. Environ. Res.*, **28**, 326e332 (2018); https://doi.org/10.1016/j.serj.2018.09.002
19. D.K. Dewi, V.M. Putri, V. Febriyanti and D.C.S. Yudha, *Equilibrium J. Chem. Eng.*, **8**, 087 (2023); https://doi.org/10.20961/equilibrium.v7i1.74484
20. A. Razak, N.M. Isa, S. Kinit and S. Adzila, *EVERGREEN J. Novel Carbon Resour. Sci. Green Asia Strat.*, **10**, 782 (2023); https://doi.org/10.5109/6792828
21. R.O. Zonato, B.R. Estevam, I.D. Perez, V.A.S. Ribeiro and R.F. Boina, *Clean. Chem. Eng.*, **2**, 100023 (2022); https://doi.org/10.1016/j.clce.2022.100023
22. A. Basit, Z. Yaqoob, A. Zahid, S. Ali, B. Shoukat, A. Khaliq, M.T. Chughtai, R. Batul, M.A.U. Rehman and S.W. Husain, *Heliyon*, **11**, e41063 (2025); https://doi.org/10.1016/j.heliyon.2024.e41063
23. N.L. Bih, M.J. Rwiza, A.S. Ripanda, A.A. Mahamat, R.L. Machunda and J.W. Choi, *Heliyon*, **11**, e41150 (2025); https://doi.org/10.1016/j.heliyon.2024.e41150
24. H. Ouaddari, B. Abbou, I. Lebkiri, A. Habsaoui, M. Ouzzine and R.F. Allah, *Chem. Phys. Impact*, **8**, 100405 (2024); https://doi.org/10.1016/j.chphi.2023.100405
25. R.K. Adday and H.M. Flayeh, *Al-Khwarizmi Eng. J.*, **21**, 23 (2025); https://doi.org/10.22153/kej.2025.02.002
26. Y.C. Sharma, Uma and S.N. Upadhyay, *Can. J. Chem. Eng.*, **89**, 377 (2011); https://doi.org/10.1002/cjce.20393
27. P.S. Kumar, R.V. Abhinaya, K.G. Lashmi, V. Arthi, R. Pavithra, V. Sathyaselvabala, S.D. Kirupha, and S. Sivanesan, *Colloid J.*, **73**, 651 (2011); https://doi.org/10.1134/S1061933X11050061
28. D. Balarak, J. Jaafari, G. Hassani, Y. Mahdavi, I. Tyagi, S. Agarwal and V.K. Gupta, *Colloid Interface Sci. Commun.*, **7**, 16 (2015); https://doi.org/10.1016/j.colcom.2015.11.004
29. G. Patel, V. Diwan and S.K. Sar, *Next Nanotechnol.*, **9**, 100464 (2026); https://doi.org/10.1016/j.nxnano.2026.100464
30. J. Wang, X. Li, Y. Fang, Q. Huang and Y. Wang, *Colloid. Surf. A Physicochem. Eng. Asp.*, **742**, 140419 (2026); https://doi.org/10.1016/j.colsurfa.2026.140419
31. G. Zou, N. Zou, Y. Tan, H. Xiao, Q. Cheng, Z. Liu, K. Wang, J. Zhu, F. Yang, D. Dua and Y. Chen, *Environ. Sci.: Processes Impacts*, **27**, 3875 (2025); https://doi.org/10.1039/D5EM00659G